16th World Conference on Earthquake Engineering, 16WCEE 2017
Santiago Chile, January 9th to 13th 2017
Paper N° 4421
Registration Code: S-O1463315219

REVISITING SARMA'S METHOD FOR SEISMIC RESPONSE OF EMBANKMENTS: FIRST RESULTS

C. Durand[(1)], E. Chaljub[(2)], P.-Y. Bard[(3)] , L. Baillet[(4)], J.-J. Fry[(5)], R. Granjon[(6)], F. Renalier [(7)]
[(1)] *PhD student, geophyConsult, France, capucine.durand@univ-grenoble-aples.fr*
[(2)] *Researcher, University Grenoble Alpes, ISTerre/CNAP, France, emmanuel.chaljub@univ-grenoble-aples.fr*
[(3)] *Researcher, University Grenoble Alpes, ISTerre / IFSTTAR, France, pierre-yves.bard@univ-grenoble-aples.fr*
[(4)] *Researcher, University Grenoble Alpes, ISTerre, France, laurent.baillet@univ-grenoble-aples.fr*
[(5)] *Expert engineer, Electricité de France, Centre d'Ingénierie Hydraulique, France, jean-jacques.fry@edf.fr*
[(6)] *Engineer, Compagnie Nationale du Rhône, France, r.granjon@cnr.tm.fr*
[(7)] *Engineer, geophyConsult, France, florence.renalier@geophyconsult.com*

Abstract

Given the very large length of embankments along rivers and channels, there is a need for a reliable, simple and affordable method to assess the stability of these structures in case of earthquake. However, most of the existing simplified methods have been developed considering earth dams. They are usually not representative in terms of height and frequency range of the particular case of a river embankment. Moreover, the river embankments do not lie directly on the rigid bedrock but on a (soft or stiff) soil foundation. For this last reason, and because it provides an analytical formulation, the Sarma's method is considered as the first simplified method to apply for assessing the dynamic response of a river embankment. However, it is based on several assumptions that have never been qualified. Therefore, in order to assess the reliability of this method, it is applied on 18 configurations of embankments and soil foundation loaded by 26 accelerograms. The results are compared with those obtained by direct numerical simulation with the spectral element method for the same configurations. The comparisons show that Sarma's simplified method generally leads to an overestimation of the peak response of the embankment. The discrepancies are mostly explained by the less accurate predictions of higher modes with Sarma's method and by the assumption of a rigid bedrock under the foundation layer. Moreover, an analysis of the strain distribution indicates that Sarma's (1979) assumption of a uniform damping in the embankment and the foundation layer is far from being always justified, especially for equivalent linear computations. Finally, the main perspectives of this work is to provide an affordable methodology to estimate the peak response of an embankment taking into account the interaction with the underlying soil, which may be more complex than a simple horizontal layer.

Keywords: embankment, dyke, levee, seismic response, simplified method, site effect.

1. Introduction

Given the very large length of existing embankments along rivers and channels, simplified methods to assess their seismic stability are necessary to save money and time. Lots of methods have already been developed for studying earth dams [1-5], but they usually appear not to be transposable to small dykes. Apart from the difference in terms of range of resonance frequencies, one of the main distinction lies in the fact that embankments are almost never overlying directly on a bedrock. For this last reason, Sarma's simplified method [2] appears to be the first method to apply on the particular case of dykes. This model takes into account the interaction between the dam and its foundation, which consists in a layer of soil underlain by the bedrock. Besides, because it is based on an analytical formulation, it can give directly the response of the system in time-domain without the additional approximations of abacus. However, Sarma's simplified method relies on several assumptions that never been qualified. The present study aims at comparing the results given by Sarma's approach with those obtained by numerical analysis in order to better constrain the possible error introduced by the assumptions. For this purpose, 18 configurations of embankments and foundations are considered. Their peak response to a set of 26 accelerograms (fitted on design spectra) calculated numerically with a two-dimensional spectral element method are compared with the one given by Sarma's equations [2].

2. Sarma's method (1979)

S.K. Sarma developed the well-known design curves for the assessment of the dynamic stability of the slopes of a dam [2]. These curves, frequently applied by geotechnical engineers, are based on the analytical resolution of the problem. The equations obtained in this way were then used by Sarma (1979) for different standard cases in order to develop the design curves. The different steps used by Sarma (1979) to solve analytically the problem consist in the estimation of:

- the inertia forces generated in the dam during the earthquake;

- the resistance of the dam against these forces;

- the consequences (irreversible displacement) when the resistance is not sufficient.

From the first point is deduced, in particular, an abacus that gives the seismic coefficient for different geometries of sliding wedges. The revisiting on Sarma's method presented in this paper concerns only the estimation of inertia forces. Moreover it is not based on the design curves deduced by Sarma (1979) but on the analytical resolution itself. This analytical resolution of the dynamic response of a dam resting on a layer is based on several assumptions listed hereinafter. The other subsection deals with the equations obtained by Sarma (1979) after the resolution of the system.

2.1 Assumptions

Sarma (1979) made the following assumptions to translate the problem into a system of equations and solve it:

- the dam is assimilated to a triangular wedge, symmetrical with respect to the vertical axis, with a length much greater than its height (so it can be studied only in two-dimensions);

- the dam is supposed to be homogeneous;

- the foundation is modeled as a horizontal layer, without any lateral variations, in only one dimension;

- the foundation layer is supposed to be homogenous, with characteristics that can be different from the properties of the dam;

- the foundation layer is resting on a semi-infinite and rigid bedrock where the horizontal input motion is applied;

- the behavior of the materials in the dam and the layer of soil stays in the linear viscoelastic domain, the only source of energy dissipation comes from the viscous damping (no radiation of energy in the rigid bedrock);

- the viscous damping is constant, does not depend on the frequency and is the same in the dam and in the layer;

- a shear beam approach is considered, thus, only horizontal displacements and simple shearing deformations are supposed to take place, moreover strains are assumed to be uniformly distributed along horizontal planes for a given depth.

The real problem is therefore simplified to a one-dimensional study.

These hypotheses can lead to several interrogations. First of all, Ambraseys (1960) shows that when the length of the crest of the dam is less than 10% of its total width, its section can be assimilated to an untruncated triangle [6]. However, it is not often the case, especially for the particular case of embankments. Moreover, in reality, lateral variations of the materials can be expected in the embankment and the foundation. Vertical variations are also possible, especially in a layer with a significant depth. Besides, the radiation damping is not taken into account because of the rigid bedrock. This can lead to an overestimation of the surface motion. Finally, concerning the shear beam solution, it has been shown that neglecting the vertical motion of a dam could give rise to a spurious overestimation of its stiffness, more particularly at high frequencies [7].

2.2 Equations giving the dynamic response

The dynamic response is assessed by adding the contributions of all the modes of the system. The n^{th} resonance pulsation ω_{0n} is given by equation (1). In this equation, $\bar{a}_n$ is the n^{th} root of equation (2), Vs_1 is the shear wave velocity in the embankment and h_1 is its height. In equation (2), J_0 and J_1 are the Bessel's functions of order 0 and 1, respectively, q is the contrast in propagation time in the dam and in the layer (equation (3)) and m is the impedance contrast between the dam and the layer (equation (4)). In equations (3) and (4), Vs_2 is the shear wave velocity in the layer, h_2 is its thickness, ρ_1 and ρ_2 are respectively the mass density in the embankment and in the foundation.

$$\omega_{0n}=\frac{\bar{a}_n V_{s1}}{h} \; ; \; \frac{J_0(\bar{a}_n)}{J_1(\bar{a}_n)}=m\tan(q\,\bar{a}_n) \qquad (1) \; ; \; (2)$$

$$q=\frac{Vs_1}{Vs_2}\frac{h_2}{h_1} \; ; \; m=\frac{Vs_1}{Vs_2}\frac{\rho_1}{\rho_2} \qquad (3) \; ; \; (4)$$

The corresponding modal shape are given by equations (5) and (6). In these equations, Φ_n and Ψ_n are the modal shapes of the embankment and of the foundation, respectively, y is the depth from the crest, P_0 and M_0 are given by equations (7) and (8).

$$\Phi_n(y)=\frac{2J_0\left(\frac{\bar{a}_n y}{h}\right)}{\bar{a}_n P_0(q,m,n)} \; ; \; \Psi_n(y)=\frac{2M_0(y)}{\bar{a}_n P_0(q,m,n)} \qquad (5) \; ; \; (6)$$

$$P_0(q,m,n)=\frac{J_1(\bar{a}_n)}{\cos(q\bar{a}_n)}(\cos^2(q\bar{a}_n)+mq+m^2\sin^2(q\bar{a}_n)-\frac{m}{\bar{a}_n}\sin(q\,\bar{a}_n)\cos(q\bar{a}_n) \qquad (7)$$

$$M_0(q,m,n,y)=\frac{mJ_1(\bar{a}_n)}{\cos(q\bar{a}_n)}\sin(q\bar{a}_n\,\frac{(h_1+h_2)-y}{h_2}) \qquad (8)$$

Finally, the absolute accelerations in the embankment $\ddot{u}_1(y,t)$ and in the layer $\ddot{u}_2(y,t)$ are given by equations (9) and (10). In these equations, n in the n^{th} mode, N is the number of modes taken into account [Sarma (1979) proposes to consider N as the total number of modes below 20Hz], t is the time, $\ddot{g}(t)$ is the input acceleration and $S_{an}(t)$ is the absolute acceleration of a single degree of freedom oscillator of pulsation ω_{0n} and viscous damping λ submitted to the accelerogram $\ddot{g}(t)$ (equation (11)). In equation (11), ω_n is the damped circular frequency and S_{dn} is the Duhamel's integral, that gives the relative displacement response of the same oscillator.

$$\ddot{u}_1(y,t)=\sum_{n=1}^{N}\Phi_n(y)S_{an}(t)+\ddot{g}(t)\left(1-\sum_{n=1}^{N}\Phi_n(y)\right) \quad (9)$$

$$\ddot{u}_2(y,t)=\sum_{n=1}^{N}\Psi_n(y)S_{an}(t)+\ddot{g}(t)\left(1-\sum_{n=1}^{N}\Phi_n(y)\right) \quad (10)$$

$$S_{an}(t)=\frac{d^2S_{dn}}{dt^2}=-(\omega_n^2-\lambda^2\omega_{0n}^2)\,S_{dn}+2\lambda\,\omega_{0n}\int_0^t\ddot{g}(t-\tau)\cos\left(\omega_n(t-\tau)\right)d\tau \quad (11)$$

3. Methodology

This study is based on the comparison between the predictions of the peak response of an embankment with Sarma's formulation and with a 2D viscoelastic numerical model. The numerical model is considered as the reference one – even if it is still an approximation of the reality. Several configurations, all based on the same standard model, of an embankment resting on a soil layer are taken into account for the comparison, they are described in the paragraph below. Apart from the extra hypotheses imposed by the Sarma's method, the Sarma's equations are applied on the same configurations as the numerical ones.

3.1 Considered embankment/soil layer configurations

Some simplifying approximations are made to define a standard model from which the characteristic parameters can vary from one configuration to another. First of all, the behavior of the embankment and its foundation are considered viscoelastic and the substratum purely elastic. The chosen standard model consists in a symmetrical, trapezoidal embankment resting on a one-dimensional horizontal layer of soil; the substratum is reached below this layer (see Fig. 1). Therefore, the geometric parameters of a standard model are:

- h_1, the height of the embankment;
- L, the width at crest of the embankment,
- f=H:V, the slope batter of the embankment,
- h_2, the thickness of the foundation layer.

The embankment is considered as homogeneous, with a uniform elastic shear wave velocity designated as Vs_1, a density ρ_1, a viscous damping ζ_1 and a Poisson's ratio called ν_1. As the compaction of the soil in the foundation usually increases with depth, the following gradient of shear wave velocity is taken into account in the layer:

$$Vs_2(z) = Vs_a + (Vs_b - Vs_a)\sqrt{\frac{z - z_a}{z_b - z_a}} \quad (12)$$

In equation (12),

- Vs_2 is the elastic shear wave velocity in the layer of foundation;
- Vs_a and Vs_b are the shear wave velocities at depths z_a and z_b respectively;
- z is the elevation (z = 0m corresponds to the top of the layer);
- z_a = 0m and z_b = -1000m.

The Poisson's ratio ν_2, the viscous damping ζ_2 and the density ρ_2 in the layer of soil are considered constant.

For this first study, only one embankment made of alluvium is considered, with a height of 10m, a crest width of 6m and a slope ratio of 2.2H:1V. The elastic shear wave velocity in the embankment is fixed at 300 m/s with a Poisson's ratio equal to 0.25 (i.e., V_P = 520 m/s) and a mass density of 2200 kg/m^3. In total, 18 case studies of

foundation layers are taken into account, corresponding to 6 different thicknesses – 3m, 10m, 30m, 100m, 300 and 900m – and 3 different profiles of elastic shear wave velocity. These profiles, defined from equation (12), are chosen in order to get three values of the mean shear wave velocity in the first 30m (Vs_{30}) – 125 m/s, 250 m/s and 500 m/s –, defined by equation (13) :

$$Vs_{30} = \frac{30}{\int_0^{30} \frac{dZ}{Vs_2(Z)}} \tag{13}$$

The characteristics of the velocity profiles in the layer are given in Table 1 and the velocity gradients are shown in Fig. 1. The Poisson's ratio in the layer is always equal to 0.25 and the mass density is kept equal to 2200 kg/m^3 for all the models. A constant (in space and frequency) viscous damping of 2.5% is considered in the layer and the embankment for all the models. Finally, in the substratum, the elastic shear wave velocity is fixed at 800 m/s with a Poisson's ratio of 0.25 and a density of 2500 kg/m^3. The geometry and the chosen parameters are summarized in Fig. 1.

Fig. 1 also shows the three possible sliding blocks considered for the study. All the blocks start from the middle of the crest, the height of block 1 is equal to half the height of the embankment, the height of block 2 is equal to the height of the embankment, and block 3 goes through the layer of foundation (at a depth corresponding to 20% of the height of the embankment, i.e., 2 m), with a maximum lateral extension of 36.4m (about 1.45 times the half width of the base of the embankment).

Table 1. Characteristics of the 3 velocity gradients considered in the layer of soil. For the two first cases, the S-wave velocity in the topmost part of the layer is lower than that of the embankment.

Vs_{30} (m/s)	**125**	**250**	**500**
Vs_a (m/s) at z=0m	80	160	434
Vs_b (m/s) at z=-1000m	480	950	1000

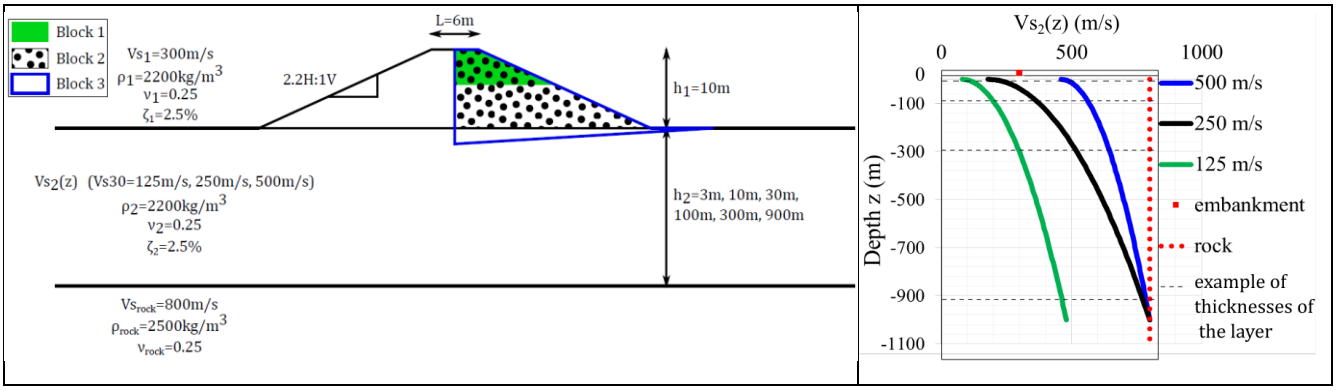

Fig. 1 – Geometry, parameters and velocity gradients.

3.2 Input accelerograms

Horizontal accelerograms fitted on French design spectra (based on Eurocode 8) are imposed as input in the numerical models and Sarma's equations in order to consider different levels of loading. Four design spectra are used Z4A to Z4D (see Fig. 2), and, for each of them, six or seven real accelerograms are selected and adjusted to represent them. They correspond to earthquakes with magnitude ranging from 4 to 6.5, depending on the spectra. In total, each embankment-soil configuration is loaded with 26 different accelerograms.

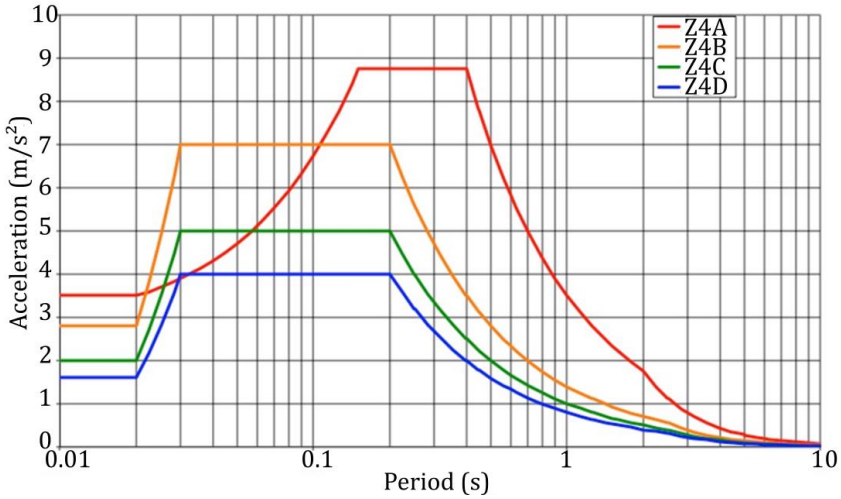

Fig. 2 – Design spectra considered for the study

3.3 Numerical analysis

The 2D spectral-element solver SPECFEM2D [8] is used for the direct numerical computation of the seismic response of the embankment. The code implements the spectral element method in space, with a polynomial order N=4, and a second order explicit finite-difference method in time. The total width of the computational domain is 2000m, with the embankment in the middle, and it extends to an elevation of -1500m (an elevation of 0m corresponds to the top of the soil foundation layer). The spectral element mesh is made of quadrangles. The mesh resolution in the layer of soil is adapted to the value of Vs_{30} in order to ensure that the results can be acceptable until 30Hz, that leads to the size of the elements to be smaller than the minimum seismic wavelength. In all models, the input motion is introduced as a plane wave with vertical incidence, imposed at the elevation -1200m. The polarization of the imposed motion coincides with the horizontal in-plane direction (SV wave). The impulse response of the 18 models is computed up to a frequency of 30Hz, and then convolved with the 26 accelerograms.

Numerous points, called receivers, are defined in the model to extract the impulse response. There are:

- a receiver every 1m on the symmetry axis, from the top of the embankment down to the rock;

- a line of receivers every 1m in depth inside the embankment (the first line on the crest and the last one at the base), with, for each line, 14 receivers distributed from the symmetry axis to the limit of the slope;

- a line of receivers every 1m in depth within the topmost part of the foundation (the first line at z=0m and the last one at z=-15m), with for each line, 21 receivers distributed every 2m (horizontal distance between two consecutive receivers).

At each receiver, the following results are extracted:

- horizontal and vertical velocities,

- the four spatial derivatives of displacements: $\frac{\partial u_x}{\partial x}(x_i,z_i,t)$; $\frac{\partial u_z}{\partial z}(x_i,z_i,t)$; $\frac{\partial u_x}{\partial z}(x_i,z_i,t)$ and $\frac{\partial u_z}{\partial x}(x_i,z_i,t)$; where x_i,z_i are the horizontal and vertical coordinates of the receiver number i, u_x and u_z are respectively the horizontal and vertical displacements, x and z are respectively the horizontal and vertical directions.

The accelerations and the horizontal shear strains are deduced from these output data.

The computations are convolved at each of these points with the chosen accelerograms (these reference accelerograms correspond to outcropping bedrock and are divided by two to account for the free surface effect for the vertically incident plane wave), in order to obtain the response of the system to these input solicitations.

3.4 Details on the application of Sarma's equations

For each of the defined models, equations (1) to (11) found by Sarma (1979) are used to assess the acceleration at each depth in time domain. These equations cannot take into account the gradient of shear wave velocity in the layer of soil. Therefore, the Vs_{30} values are used in this case. The 26 accelerograms at outcropping bedrock are directly used as input accelerograms for all of the 18 configurations. As, with the Sarma's method, there is no lateral variations of the results, the accelerations in time domain are deduced every 1m (vertical distance between two calculation points).

4. Results

4.1 Horizontal shear strains obtained with numerical models

The shear strains at each receiver of the numerical models are deduced from the output data for all the accelerograms. For each receiver, the maximum value reached during the whole dynamic response of the system is calculated (the maxima are not necessarily synchronous at all the receivers). For a given spectra, the mean of the maximum shear strains on the six or seven corresponding accelerograms are determined for each receiver. The results are interpolated between receivers in order to get images of the peak shear strains such as in Fig.3.

Fig.3(a) and Fig.3(b) map the peak shear strains for the same geometry and the same input solicitation, the only difference resides in the properties of the layer: in Fig.3(a), the layer is softer (Vs_{30} = 125 m/s) than in the second case (Vs_{30} = 500 m/s). There is a factor of 10 in the peak shear strain between the two cases. The differences can be better seen in Fig.3(c) which represents the profile of peak shear strains on the symmetry axis for the same two cases. One can see that the localization of the maxima are not the same in the two situations:

- when the layer is softer than the embankment, all the deformations are concentrated inside it, and the embankment only follows the motion of its foundation with a quasi-uniform deformation;

- on the contrary, when the layer is stiffer than the embankment, the peak deformation is rather located in the heart of the embankment, and more especially near its bottom part close to the velocity contrast with the foundation soil.

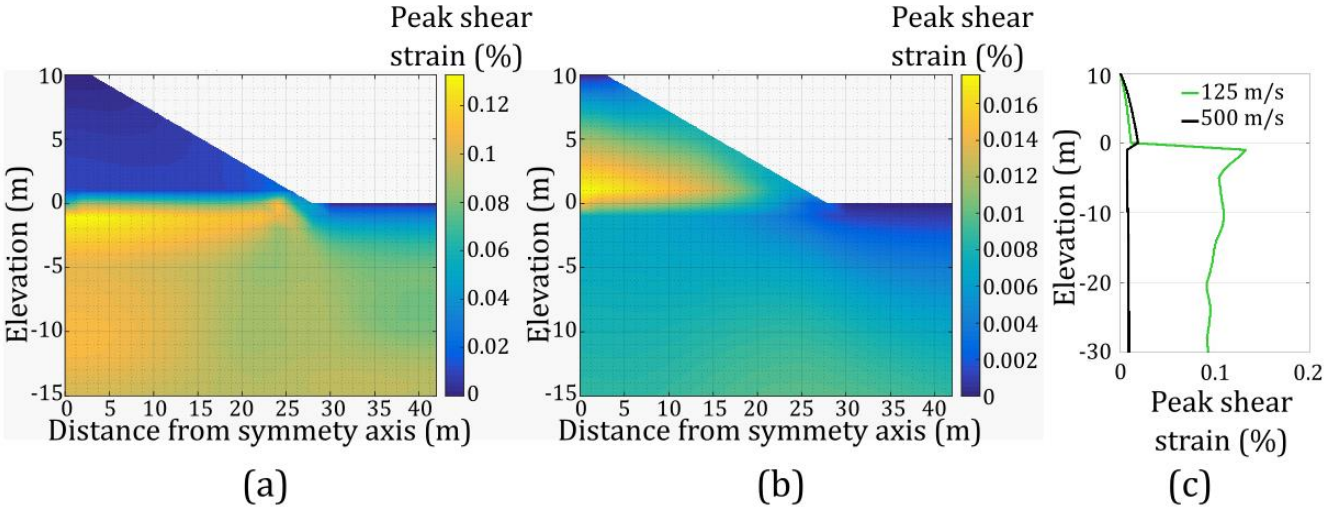

Fig.3– (a) and (b): Peak shear strains (%) reached in the case of a layer of 30m, with a Vs_{30} equal to 125 m/s (a) and 500 m/s (b), and a PGA of the input accelerogram equal to 2.8 m/s² (spectrum Z4B on Fig. 2).
(c) : Comparison of the peak shear strains reached on the symmetry axis for these two cases.

One can notice that the maximum values of strains reached inside the embankment are globally at the same values in the two cases. This might mean that, for a given loading level, the deformation is controlled by the value of the shear modulus, which stays the same in the embankment for all the models used in this study. As damping is strongly related to shear deformation in all non-linear constitutive models, for strong loading, the assumption of Sarma (1979) that the viscous damping is the same in the layer and the embankment in any case does not seem

realistic. To the advantage of the shear beam approach, the shear strains seem to remain generally the same for a given depth.

4.2 Horizontal accelerations obtained with numerical models and the equations of Sarma (1979)

The horizontal accelerations are derived from the velocities at each receiver of the numerical models, in particular along the symmetry axis. As for the shear deformation, the maximum value is deduced at each point, and the mean of the response to the six or seven accelerograms of a given design spectra is calculated. The Sarma's equations are used to derive the time-acceleration at each depth. In the same manner, the maximum reached at each depth (not necessarily synchronously) is deduced, and the mean is made on the accelerograms of a given design spectra. The figures Fig.4 presents the evolution of these maxima for different models.

Looking at the numerical results in Fig.4(a), one can see that a very thin (3m), soft layer (Vs_{30}=125 m/s) amplifies significantly the input. On the top of this thin and soft layer, the embankment seems to follow the motion of its foundation without amplifying it so much. When the layer is harder (Vs_{30}=500m/s, in blue) than the embankment (V_1=300 m/s), the layer does not amplify any more the input solicitation, whereas the embankment increases it by a factor 2.7. These observations are also visible on the results obtained with the Sarma's method. However, the dynamic response given by Sarma's method are, in this case, globally overestimated:

- when the layer is softer than the embankment, the amplification of the motion by the layer is overestimated whereas the amplification by the embankment is globally the same as the one obtained with Specfem;

- when the layer is harder than the embankment, the amplification of the motion by the layer is well predicted whereas the amplification by the embankment is overestimated.

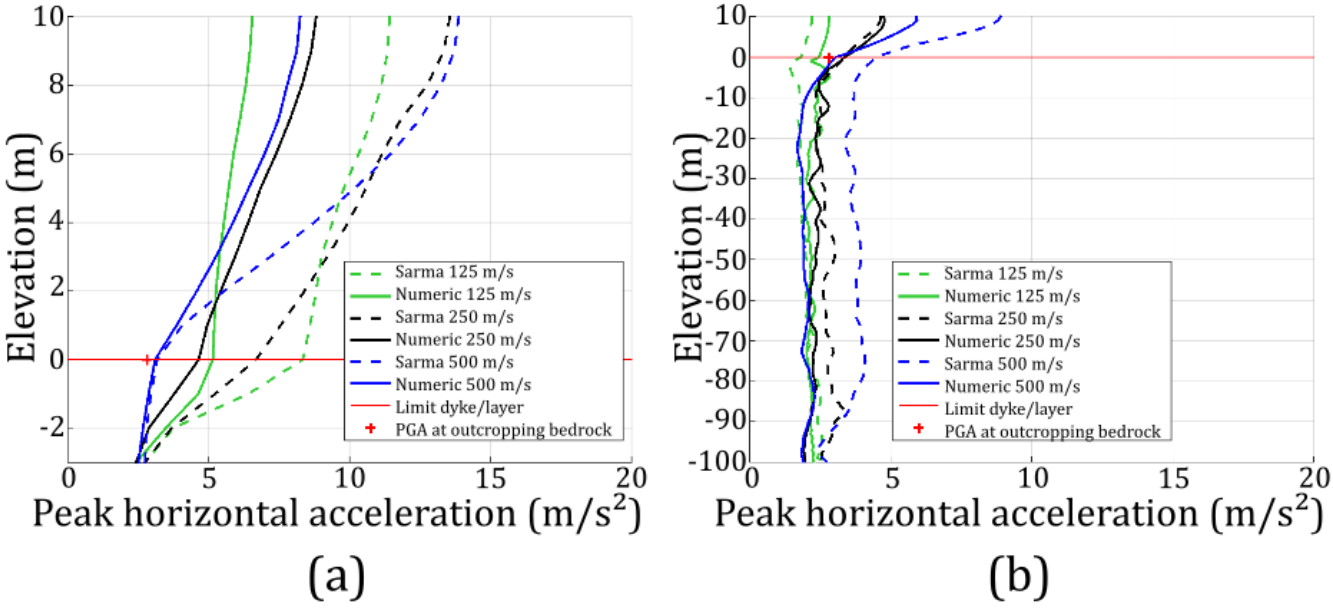

Fig.4 – Evolution with depth of the peak horizontal acceleration reached with Specfem model (on the symmetry axis) and with the formulation of Sarma (1979) for a PGA of the input solicitation equal to 2.8 m/s² (spectrum Z4B on Fig. 2) and a thickness of the layer equal to 3m (a) and 100m (b).

The first point may be explained by the assumption of an infinite impedance contrast at the interface between the layer and the bedrock. The second point is in agreement with the conclusion of Gazetas (1987), who compared the results obtained with a two dimensional finite element analysis to those obtained with a shear beam approach. One of the conclusions from this study is that the shear beam approach leads to an overestimation of the acceleration at crest [7]. According to Gazetas (1987), this discrepancy can be explained by the greater importance given to high frequency content of the motion, which is the consequence of neglecting its vertical component. Sarma's

method is less accurate for the prediction of higher modes because they affect more the vertical motion. This phenomenon is not visible for a soft layer that filters out the high frequencies.

Fig.4(b) represents the case of a deeper layer (100m); the observations are not exactly the same. Having a look at the numerical results, the common point with the case of a thin layer is that the harder the foundation the higher the amplification by the embankment and the crest motion. When the mean velocity in the first 30m is equal to 250 m/s or 500 m/s, there is no amplification inside the layer because it is relatively stiff. However, in the case of a soft layer (Vs_{30}=125m/s), one can observe that the layer attenuates the input motion. This is caused by the relatively high viscous damping in the model (2,5%) combined with the lower wavelength. Like in Fig.4a, the results obtained with Sarma's equations catch relatively well the same phenomenon. Regarding the response of the embankment, the same remark can be done: when the layer is softer than the embankment, the amplification of the motion by the embankment is well predicted. Nevertheless, the attenuation by a soft layer and the amplification by a stiff layer are overestimated in this case. The main differences between the case of a thin and a thick layer that might explain the modification of the predicted response of the layer with Sarma's equations are the greater importance of the viscous damping and of the velocity gradient with a thicker layer. A phenomenon which is more visible in Fig.4(b) than in Fig.4(a) is the differences in peak accelerations at the basis of the layer between Sarma and Specfem. This comes from the different ways of introducing the input motion and from the assumption of a rigid bedrock in Sarma (no radiation of energy through the bedrock).

4.3 Quantification of the error introduced by Sarma's resolution on the maximum acceleration at crest

In order to study the inaccuracy introduced by the shear beam approach for the estimation of maximum acceleration at crest, the following ratio is calculated for all the situations:

$$R_{A_{crest}} = \frac{Amax_{crest_{SARMA}}}{Amax_{crest_{SPECFEM}}} \quad (14)$$

In equation (3), $Amax_{crest_{SARMA}}$ and $Amax_{crest_{SPECFEM}}$ are the peak horizontal accelerations at the crest of the embankment, on the symmetry axis, with Sarma's formulation and numerical calculation respectively.

The mean value of this ratio, calculated on the 18 models and the 26 input motions, is equal to 1.33 with a logarithmic (with a base 10) standard deviation equal to 0.37. In order to study the relative impact of the different parameters the mean ratio is calculated for a given design spectra, a given thickness of the layer and, finally, for a given Vs_{30} of the layer (Fig.5). In this figure the mean and the logarithmic standard deviation obtained in each case are represented. The reference (in red) is the results considering all cases (mean of 1.33 with a logarithmic standard deviation equal to 0.37).

As one can see in Fig.5(a), the overestimation of acceleration at crest is of the same order (between 35% and 40%) for design spectra Z4B, Z4C and Z4D that have globally the same frequency content (but different peak ground acceleration). The overestimation is twice less important when the input motion is fitted on the design spectra Z4A, which has more energy at low frequency. This also tends to confirm that Sarma's equations do not lead to a satisfying prediction of the motion at higher frequencies.

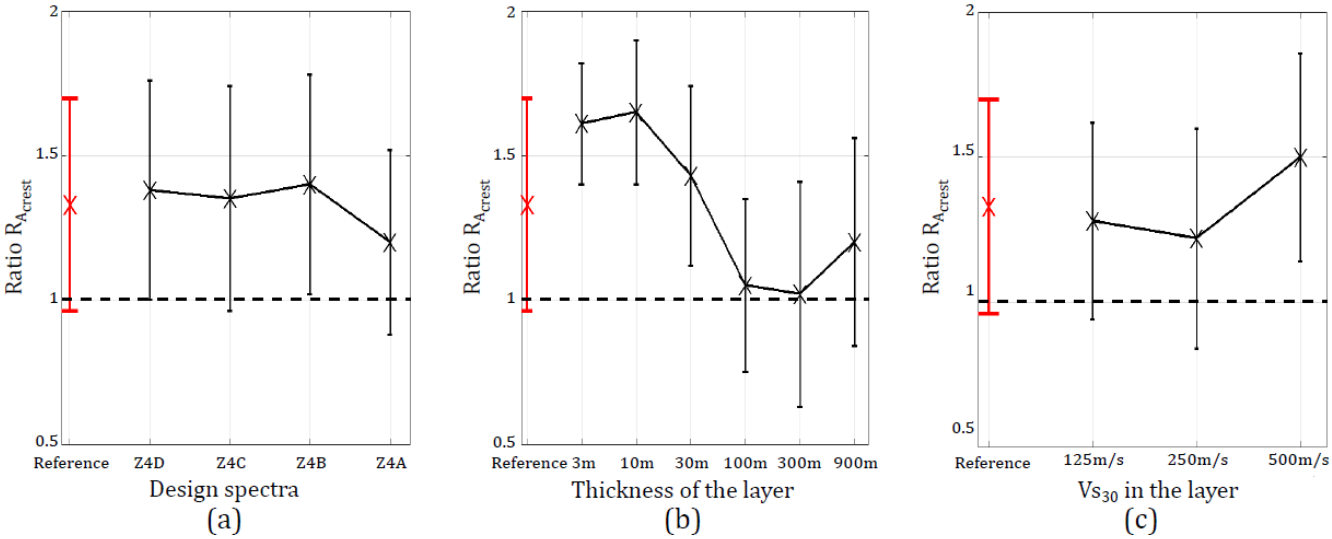

Fig.5 – Mean and standard deviation of ratio of peak acceleration at crest, and their variations with respect to design spectra (a), thickness of the layer (b) and Vs_{30} in the layer (c).

Fig.5(b) shows the evolution of the ratio $R_{A_{crest}}$ with respect to the thickness of the layer of foundation. The results are a generalization of what has been observed in paragraph 4.2 for the specific cases of a layer of 3m and 100m, with larger overestimations (up to 60%) for thin layers. Because of viscoelasticity, a large thickness of the layer tends to attenuate the high frequency content of the motion, and therefore to reduce the overestimation amplification at crest with Sarma's method. However, it is not the case for the extreme case of a 900 meters thick layer, maybe because of the bigger importance of the velocity gradient for such a big thickness.

Finally, as seen in paragraph 4.2, the ratio $R_{A_{crest}}$ is of the same order of magnitude (20 to 30 % of overestimation) when the layer is softer than the embankment whereas, for a Vs_{30} value equal to 500 m/s in the foundation, the acceleration at crest is generally overestimated by 50% (Fig.5(c)). This is consistent with results mentioned in Gazetas (1987), who compared the shear beam formulation with a two-dimensional finite element analysis: he found, for the shear beam approach, a mean overestimation about 50% of the peak acceleration at crest of a dam resting on an elastic bedrock (impedance contrast between the dam and the bedrock equal to 0.2).

4.4 Quantification of the error introduced by Sarma's resolution on the peak acceleration of potential sliding blocks.

The peak acceleration at crest is not the best indicator of the possible damage that can be generated on the embankment: irreversible displacements occur when the resistance mobilized along a sliding surface is not sufficient (smaller than the inertia forces endured by the block) to prevent the sliding. Therefore the ability of Sarma's method to estimate the peak acceleration on three possible sliding blocks (defined in Fig. 1) is studied by comparison with the values obtained with Specfem. Considering the numerical results, the acceleration endured by each block B_k (k = 1,3) is derived in time domain from the acceleration at each receiver (synchronous mean on the whole area of the block at each time step t) for each situation (model and accelerogram). The peak value is called $Amax_{Bk_{SPECFEM}}$. About Sarma's method, the acceleration of a possible sliding block is derived from the acceleration at each depth, considering that it is uniform for a given depth (synchronous mean on the delimited block, in time-domain). The peak value is called $Amax_{Bk_{SARMA}}$. For each block B_k and each situation (model and design spectra), the following ratio is considered:

$$R_{A_{Bk}} = \frac{Amax_{Bk_{SARMA}}}{Amax_{Bk_{SPECFEM}}} \quad (15)$$

The mean value of this ratio, considering all the models and all the accelerograms, is equal to 1.40 for block 1, 1.44 for block 2 and 1.49 for block 3 with logarithmic (base 10) standard deviation respectively equal to 0.39, 0.38 and 0.39. These values are generally the same for the three blocks, however it slightly increases with block number,

probably because the lateral extent of the block also increases, giving more impact to the assumption of a uniform acceleration at a given depth. As for the peak acceleration at crest, the evolutions of the ratio $R_{A_{block\ b}}$ with respect to the design spectra, the thickness of the layer and the Vs_{30} in the layer are given on

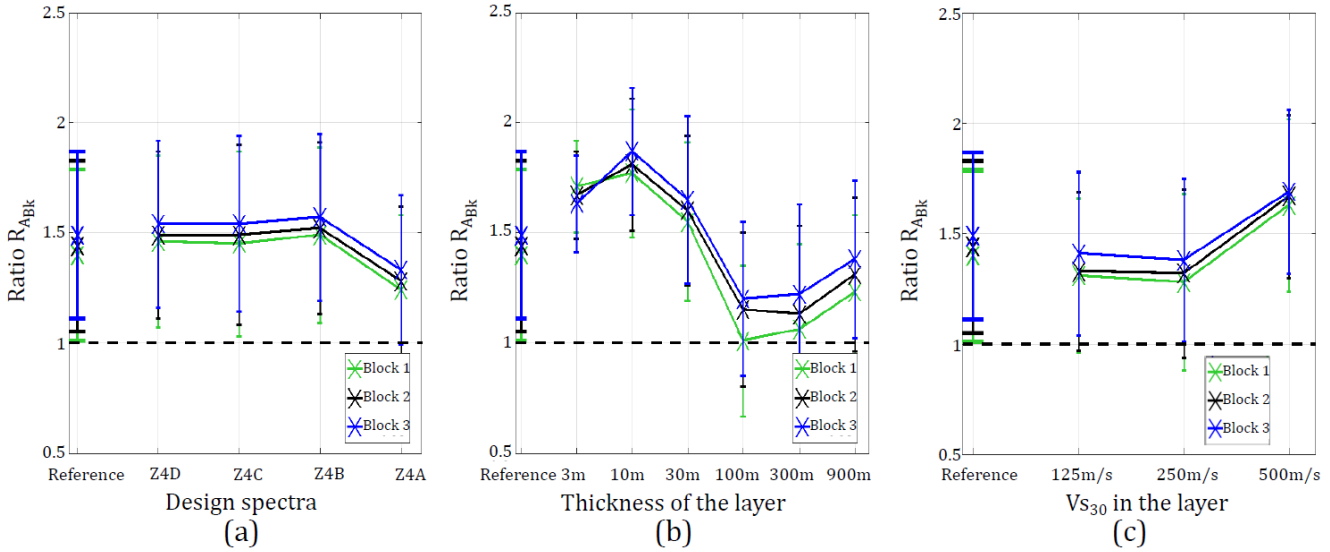

Fig. 6. On this figure, the references on left are the aforementioned mean and standard deviation values for each block.

The conclusions are the same as for peak acceleration at crest. However, one can notice that the Sarma's method generally leads to an even bigger overestimation when considering the peak acceleration of possible sliding blocks. Applying this method may lead, in several cases, to overestimate the inertia forces and therefore the resulting damages on the embankment.

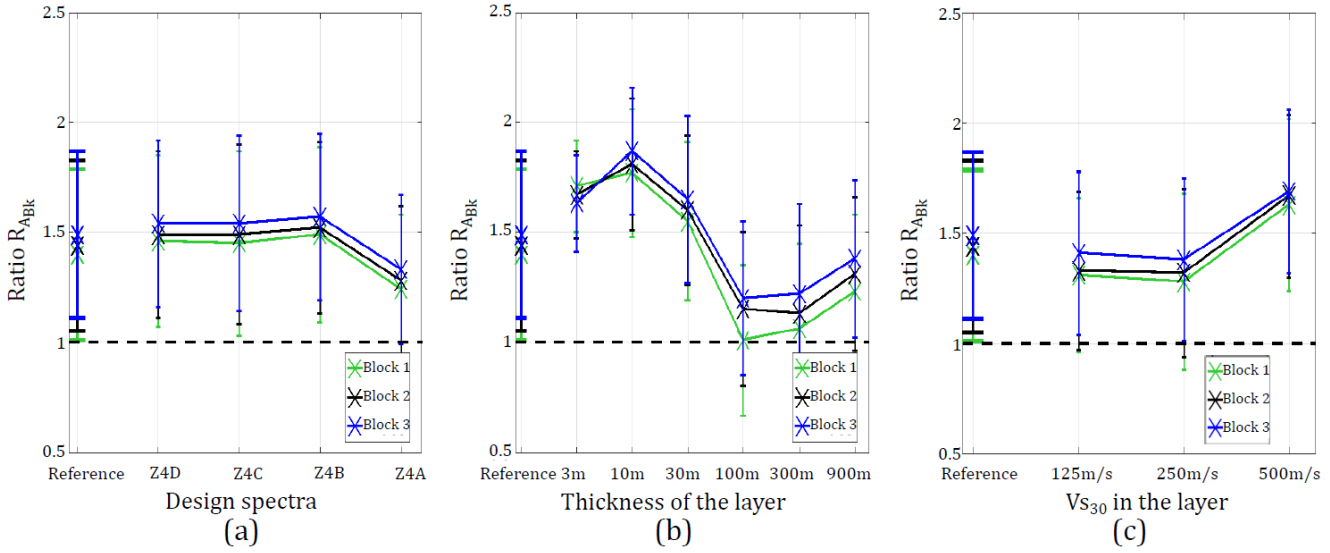

Fig. 6 – Mean and standard deviation of ratio of peak acceleration of the three blocks defined in Fig. 1, with respect to design spectra (a), thickness of the layer (b) and Vs_{30} in the layer (c).

5. Conclusions and perspectives

This study is based on the comparison of Sarma's method to a 2D finite element numerical method. The results show that Sarma's method generally tends to overestimate the maximum response of the embankment resting on its foundation. On average, the inertia forces on potential sliding blocks are overestimated by 45%: that would necessarily lead to an overestimation of the resulting irreversible displacements. This is probably mainly

due to the bad representation of the behavior of higher modes and to the assumption of a rigid bedrock. The discrepancies are also explained by the assumption of a homogeneous layer of soil that is not valid for deep soil layer. Consequently, Sarma's equations may be adapted in order to take into account a velocity gradient in the soil layer.

However, the numerical method also relies on several assumptions about the features of the embankment, the foundation and the bedrock:

- the geometry of the embankment is simplified (two-dimensional, trapezoidal section, symmetric) as well as its materials (homogeneous, viscoelastic, non-saturated);

- the geometry of the foundation is also simplified (one-dimensional, horizontal) as well as its materials (no lateral variations, viscoelastic, not-saturated);

- the viscous damping is considered to be constant and to be the same in the soil layer and the embankment;

- the input motion is on horizontal direction only.

The main problem remains the representation of the damping – which has a major effect on the results. Sarma (1979) developed design curves by using a uniform value of 20% for the viscous damping inside both the embankment and the soil layer in order to represent all sources of dissipation of energy in case of strong earthquake in a simple way. Having a look at the deformation in this study, it is not realistic to choose the same value of damping in the embankment and in the layer. Besides, such a great value is not justified considering the peak shear strains obtained here for relatively moderate motion. Another issue that needs to be investigated deals with the relevancy of the linear-equivalent approach: up to which loading level is this acceptable?

This study will be completed by taking into account more geometries of embankments, additional values of shear wave velocities in the embankment and different viscous damping in the embankment and the soil layer. In the long term, it would be also interesting to study the impact of a two dimensional valley.

6. References

[1] Makdisi FI and Seed HB (1978): Simplified procedure for estimating dam and embankment earthquake-induced deformations. *Journal of Geotechnical Engineering Division*, **104** (GT7), 849-867.

[2] Sarma AK (1979): Response and stability of earth dams during strong earthquakes. *Misc. Paper GL-79-13, Geot. Lab., US Army Engineers Waterways Experiment Receiver*, Vicksburg, USA.

[3] Ambraseys NN and Menu JM (1988): Earthquake-induced ground displacements. *Earthquake Engineering and Structural Dynamics*, **16**, 985-1006.

[4] Bray JD and Travassarou T (2007): Simplified procedure for estimating earthquake-induced deviatoric slope displacements. *Journal of Geotechnical and Geoenvironmental Engineering*, **133** (4), 381-392.

[5] Papadimitriou AG, Bouckovalas GD, Andrianopoulos KI (2014): Methodology for estimating seismic coefficients for performance-based design of earthdams and tall embankments. *Soil Dynamics and Earthquake Engineering*, **56**, 57-73.

[6] Ambrasey NN (1960): On the shear response of a two-dimensional truncated wedge subjected to an arbitrary disturbance. *Bulletin of Seismological Society of America*, **50** (1), 45-56.

[7] Gazetas G (1987): Seismic response of earth dams: some recent developments. *Soil Dynamics and Earthquake Engineering*, **6** (1), 2-47.

[8] Martin R, Komatitsch D, Blitz C, Le Goff N (2008): Simulation of seismic wave propagation in an asteroid based upon an unstructured MPI spectral-element method: blocking and non-blocking communication strategies. *High Performance Computing for Computational Science-VECPAR 2008* (pp. 350-363). Springer Berlin Heidelberg.